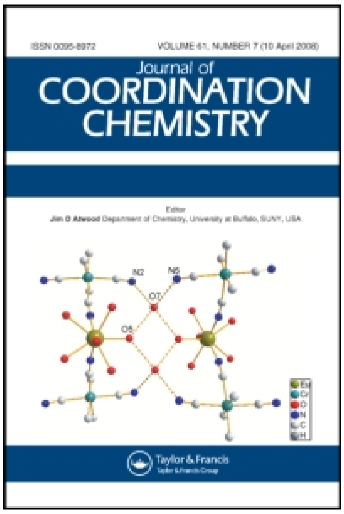

Journal of Coordination Chemistry
Publication details, including instructions for authors and subscription information:
http://www.informaworld.com/smpp/title~content=t713455674

Stereospecific interactions through <i>π</i> -conjugated systems of sulfur-bridged dinuclear Co(III)-Pd(II) and Co(III)-Pt(II) complexes of optically active penicillaminates

Yasunori Yamada[a]; Masahiko Inoue[a]; Ken-Ichi Okamoto[b]
[a] Faculty of Science and Engineering, Department of Chemistry and Applied Chemistry, Saga 840-8502, Japan [b] Department of Chemistry, Graduate School of Pure and Applied Science, Tsukuba, Ibaraki 305-8571, Japan

To cite this Article Yamada, Yasunori , Inoue, Masahiko and Okamoto, Ken-Ichi(2008) 'Stereospecific interactions through <i>π</i> -conjugated systems of sulfur-bridged dinuclear Co(III)-Pd(II) and Co(III)-Pt(II) complexes of optically active penicillaminates', Journal of Coordination Chemistry, 61: 9, 1385 — 1398

To link to this Article: DOI: 10.1080/00958970701595973

URL: http://dx.doi.org/10.1080/00958970701595973

Journal of Coordination Chemistry
Vol. 61, No. 9, 10 May 2008, 1385–1398

Stereospecific interactions through π-conjugated systems of sulfur-bridged dinuclear Co(III)-Pd(II) and Co(III)-Pt(II) complexes of optically active penicillaminates

YASUNORI YAMADA*†, MASAHIKO INOUE†
and KEN-ICHI OKAMOTO‡

†Faculty of Science and Engineering, Department of Chemistry and Applied Chemistry,
Saga University, 1 Honjo-machi, Saga 840-8502, Japan
‡Department of Chemistry, Graduate School of Pure and Applied Science,
University of Tsukuba, 1-1-1 Tennodai, Tsukuba, Ibaraki 305-8571, Japan

(*Received 17 April 2007; accepted 12 June 2007*)

The reaction of *trans*(*N*)-[Co(D-pen)$_2$]$^-$ (pen = penicillaminate) or *trans*(*N*)-[Co(L-pen)$_2$]$^-$ with [MCl$_2$(L)] (M = Pd or Pt, L = 2,2′-bipyridine (bpy) or 4,4′-dimethyl-2,2′-bipyridine (dmbpy)) stereoselectively gave an optically active S-bridged dinuclear complex, [M(L){Co(D-pen)$_2$}]Cl · 3H$_2$O or [M(L){Co(L-pen)$_2$}]Cl · 3H$_2$O. The mixture of equimolar amounts of these two enantiomers in H$_2$O crystallizes as [M(L){Co(D-pen)$_2$}]$_{0.5}$[M(L){Co(L-pen)$_2$}]$_{0.5}$Cl · *n*H$_2$O (**1c**Cl · 7H$_2$O: M = Pd, L = bpy, *n* = 7; **2c**Cl · 7H$_2$O: M = Pd, L = dmbpy, *n* = 7; **3c**Cl · 6H$_2$O: M = Pt, L = dmbpy, *n* = 6), in which the enantiomeric complex cations are included in the ratio of 1 : 1. In the crystals of **1c**Cl · 7H$_2$O, [Pd(bpy){Co(D-pen)$_2$}]$^+$ (**1a**) and [Pd(bpy){Co(L-pen)$_2$}]$^+$ (**1b**) are arranged alternately while overlapping the bpy planes along the *a* axis, and the π electronic systems of bpy moieties interact with each other. This is quite a contrast to the optically active **1a**Cl · 3H$_2$O or **1b**Cl · 3H$_2$O, which exist as monomers without intermolecular interactions. In crystals of **2c**Cl · 7H$_2$O and **3c**Cl · 6H$_2$O, similarly, the two enantiomeric complex cations interact with each other through the dmbpy frameworks. However, the interplane distances between the stacked π systems in these dmbpy complexes are considerably longer than in the bpy complexes. Such structural characteristics significantly reflect their diffuse reflectance spectra.

Keywords: Stereospecific interactions; Co(III)-Pd(II) and Co(III)-Pt(II) complexes; Bipyridine complexes; Penicillaminate complexes; Crystal structures; Spectrochemistry

1. Introduction

Octahedral metal complexes chelated by β-aminoalkylthiolates act as an S-donating bidentate metalloligand toward [MX$_2$(bpy)] (M = Pd(II) or Pt(II), X = Cl$^-$ or NO$_3^-$, bpy = 2,2′-bipyridine), in which two X$^-$ ligands are susceptible to substitution by other ligands, resulting in the formation of dinuclear complex composed of

---

*Corresponding author. Email: yyamada@cc.saga-u.ac.jp

Journal of Coordination Chemistry
ISSN 0095-8972 print/ISSN 1029-0389 online
DOI: 10.1080/00958970701595973

$[M(\mu\text{-}S)_2(bpy)]$ framework and octahedral metal unit [1–5]. For instance, *fac*(*S*)-$[Co(aet)_3]$ (aet = 2-aminoethanethiolate) reacts with $[PtCl_2(bpy)]$ to afford a dinuclear complex, $[Pt(bpy)\{Co(aet)_3\}]^{2+}$ [1]. A similar reaction of $[Ni\{Co(aet)_2(en)\}_2]^{4+}$ (en = ethylenediamine), in which the two terminal *cis*(*S*)-$[Co(aet)_2(en)]^+$ units can be regarded as bidentate S-donating metalloligands, with $[PtCl_2(bpy)]$ gives $[Pt(bpy)\{Co(aet)_2(en)\}]^{3+}$ [1]. These dinuclear complexes are obtained as racemic crystals in conformity to possible two absolute configurations, *Δ* and *Λ*, for such octahedral S-donating metal units,. In the racemic crystals, dimeric or higher dimensional linear-chain structures are constructed by π–π stacking interactions between the π frameworks. The optically active dinuclear complexes, *Λ*-$[Pt(bpy)\{Co(aet)_2(R\text{-}pn)\}]^{3+}$ (pn = 1,2-propanediamine) and *Λ*-$[Pt(bpy)\{Co(aet)_2(S\text{-}pn)\}]^{3+}$, are obtained by reactions of $[PtCl_2(bpy)]$ with *ΔΔ*-$[Ni\{Co(aet)_2(R\text{-}pn)\}_2]^{4+}$ (pn = 1,2-propanediamine) and *ΛΛ*-$[Ni\{Co(aet)_2(S\text{-}pn)\}_2]^{4+}$, respectively [3, 5]. In addition, analogous reaction of $[PtCl_2(bpy)]$ with *trans*(*N*)-$[Co(\text{D-pen})_2]^-$ (pen = penicillaminate) or $[Co(\text{L-pen})_2]^-$ also leads to formation of optically active $[Pt(bpy)\{Co(\text{D-pen})_2\}]^+$ or $[Pt(bpy)\{Co(\text{L-pen})_2\}]^+$ [3, 4]. Although such optically active dinuclear complexes exist as monomers in the crystalline states, mixtures of equimolar amounts of two enantiomers in solution crystallize as racemates, in which dimers or linear-chains are established due to π–π stacking [4, 5]. It is obvious from these facts that stereospecific interactions exist between such enantiomeric dinuclear complex cations. Furthermore, such interactions in racemic crystals result in distinguishable diffuse reflectance spectral behaviors from the monomeric optically active complexes [2–5]. For stereospecific interactions, however, there are many unclear points including the mechanism of modification in electronic nature induced by formation of dimer or linear-chain. In order to gain more information on the electronic and steric factors in square-planar units for these stereospecific interactions, we herein examine the assemblies between three types of enantiomers, $[Pd(bpy)\{Co(\text{D-pen})_2\}]^+$ and $[Pd(bpy)\{Co(\text{L-pen})_2\}]^+$, $[Pd(dmbpy)\{Co(\text{D-pen})_2\}]^+$ (dmbpy = 4,4′-dimethyl-2,2′-bipyridine) and $[Pd(dmbpy)\{Co(\text{L-pen})_2\}]^+$, and $[Pt(dmbpy)\{Co(\text{D-pen})_2\}]^+$ and $[Pt(dmbpy)\{Co(\text{L-pen})_2\}]^+$, from stereo- and spectrochemical aspects.

2. Experimental

2.1. *Materials*

2,2′-Bipyridine and $CoCl_2 \cdot 6H_2O$ were obtained from Wako Pure Chemical Ind. Co., Ltd., and Na_2PdCl_4 and K_2PtCl_4 were from Tanaka Rare Metal Ind., Ltd. 4,4′-Dimethyl-2,2′-bipyridine and L-penicillamine were purchased from Aldrich Chemical Co., Inc., and D-penicillamine was obtained from Tokyo Chemical Co., Ltd. $K[Co(\text{D-pen})_2] \cdot 2.5H_2O$, $K[Co(\text{L-pen})_2] \cdot 2.5H_2O$, $[PdCl_2(bpy)]$, $[PdCl_2(dmbpy)]$, and $[PtCl_2(dmbpy)]$ were prepared by modified methods from the literature [6–9]. $[Pd(bpy)\{Co(\text{D-pen})_2\}]Cl \cdot 3H_2O$ (**1a**$Cl \cdot 3H_2O$) was synthesized by the previously reported procedure [3], using $K[Co(\text{D-pen})_2] \cdot 2.5H_2O$ and $[PdCl_2(bpy)]$. Other chemicals were purchased from Wako Pure Chemical Ind. Co., Ltd., or Tokyo Chemical Co., Ltd. All of the chemicals were of reagent grade and used without further purification.

2.2. *Preparation of [Pd(bpy){Co(L-pen)$_2$}]Cl • 3H$_2$O (1bCl • 3H$_2$O)*

To a reddish brown solution containing K[Co(L-pen)$_2$] · 2.5H$_2$O (0.22 g, 0.5 mmol) in 25 mL H$_2$O was added [PdCl$_2$(bpy)] (0.17 g, 0.5 mmol). After the mixture was stirred at 55°C for 1 h, a saturated NaCl solution (5 mL) was added to the resulting brown solution and the solution was allowed to stand at 25°C for several days resulting in brown crystals collected by filtration. Yield: 0.25 g (71% based on Co). Anal. Calcd for $C_{20}H_{32}N_4O_7S_2ClCoPd$ (**1b**Cl · 3H$_2$O): C, 34.05; H, 4.57; N, 7.94%. Found: C, 34.08; H, 4.60; N, 7.88%. ^{1}H NMR (600 MHz, D$_2$O), $\delta = 1.61$ (s, 6H, pen), 1.91 (s, 6H, pen), 3.85 (s, 2H, pen), 7.92 (t, 2H, bpy), 8.41 (t, 2H, bpy), 8.49 (d, 2H, bpy), 9.03 (d, 2H, bpy). ^{13}C NMR (600 MHz, D$_2$O), $\delta = 30.92$ (pen), 34.52 (pen), 55.89 (pen), 75.46 (pen), 126.81 (bpy), 130.73 (bpy), 144.70 (bpy), 151.34 (bpy), 159.07 (bpy), 183.62 (pen). UV-Vis spectrum in H$_2$O [$\nu_{\max}$, $10^3\,\mathrm{cm}^{-1}$ (log ε/mol^{-1} dm^3 cm^{-1})]: 15.82 (1.85), 19.1 (2.1)$^{\text{shoulder (sh)}}$, 22.6 (2.7)$^{\text{sh}}$, 29.2 (3.8)$^{\text{sh}}$, 31.2 (4.2)$^{\text{sh}}$, 32.36 (4.23), 34.96 (4.23), 42.19 (4.64). CD spectrum in H$_2$O [$\nu_{\max}$, $10^3\,\mathrm{cm}^{-1}$ ($\Delta\varepsilon$)]: 15.92 (+2.64), 19.46 (−10.72), 22.9 (+10.4)$^{\text{sh}}$, 25.51 (+17.74), 28.25 (+21.55), 32.25 (−52.62), 35.5 (−37.0)$^{\text{sh}}$, 40.2 (−32.1)$^{\text{sh}}$, 43.10 (−50.22). Diffuse reflectance spectrum [$\nu_{\max}$, $10^3\,\mathrm{cm}^{-1}$]: 15.75, 19.0$^{\text{sh}}$, 22.4$^{\text{sh}}$, 28.5$^{\text{sh}}$, 30.58, 31.7$^{\text{sh}}$, 34.1$^{\text{sh}}$, 40.0$^{\text{sh}}$.

2.3. *Preparation of [Pd(bpy){Co(D-pen)$_2$}]$_{0.5}$[Pd(bpy){Co(L-pen)$_2$}]$_{0.5}$Cl • 7H$_2$O (1cCl • 7H$_2$O)*

To a brown solution containing **1a**Cl · 3H$_2$O (0.18 g, 0.25 mmol) in 10 mL H$_2$O was added **1b**Cl · 3H$_2$O (0.18 g, 0.25 mmol) in 10 mL H$_2$O. After the mixture was allowed to stand at 25°C for several days, the resulting brown crystals were collected by filtration. Yield: 0.34 g (87% based on Co). Anal. Calcd for $C_{20}H_{40}N_4O_{11}S_2ClCoPd$ (**1c**Cl · 7H$_2$O): C, 30.90; H, 5.18; N, 7.21%. Found: C, 30.86; H, 5.20; N, 7.15%. ^{1}H NMR (600 MHz, D$_2$O), $\delta = 1.61$ (s, 6H, pen), 1.91 (s, 6H, pen), 3.86 (s, 2H, pen), 7.92 (t, 2H, bpy), 8.41 (t, 2H, bpy), 8.50 (d, 2H, bpy), 9.03 (d, 2H, bpy). ^{13}C NMR (600 MHz, D$_2$O), $\delta = 30.92$ (pen), 34.52 (pen), 55.89 (pen), 75.45 (pen), 126.82 (bpy), 130.73 (bpy), 144.70 (bpy), 151.35 (bpy), 159.07 (bpy), 183.62 (pen). UV-Vis spectrum in H$_2$O [$\nu_{\max}$, $10^3\,\mathrm{cm}^{-1}$ (log ε/mol^{-1} dm^3 cm^{-1})]: 15.90 (1.92), 19.1 (2.1)$^{\text{sh}}$, 22.6 (2.8)$^{\text{sh}}$, 29.2 (3.9)$^{\text{sh}}$, 31.2 (4.2)$^{\text{sh}}$, 32.36 (4.31), 34.96 (4.31)$^{\text{sh}}$, 42.55 (4.72). Diffuse reflectance spectrum [$\nu_{\max}$, $10^3\,\mathrm{cm}^{-1}$]: 15.55, 20.8$^{\text{sh}}$, 28.01, 30.4$^{\text{sh}}$, 31.6$^{\text{sh}}$, 34.1$^{\text{sh}}$, 38.8$^{\text{sh}}$.

2.4. *Preparation of [Pd(dmbpy){Co(D-pen)$_2$}]Cl • 3H$_2$O (2aCl • 3H$_2$O)*

To a reddish brown solution containing K[Co(D-pen)$_2$] · 2.5H$_2$O (0.22 g, 0.5 mmol) in a 1 : 1 mixed solvent of methanol and H$_2$O (50 mL) was added [PdCl$_2$(dmbpy)] (0.18 g, 0.5 mmol). The mixture was stirred at 55°C for 1 h, whereupon it became dark brown. After cooling to ambient temperature, any unreacted materials were removed by filtration. The filtrate was evaporated to one tenth of its original volume under reduced pressure. After ca 20 mL acetone was added, the solution was allowed to stand at 25°C for several days. The resulting brown microcrystals were collected by filtration. Yield: 0.24 g (65% based on Co). Anal. Calcd for $C_{22}H_{36}N_4O_7S_2ClCoPd$ (**2a**Cl · 3H$_2$O): C, 36.02; H, 4.95; N, 7.64%. Found: C, 36.05; H, 4.96; N, 7.59%. ^{1}H NMR (600 MHz, D_2O), $\delta = 1.59$ (s, 6H, pen), 1.90 (s, 6H, pen), 2.66 (s, 6H, dmbpy), 3.85 (s, 2H, pen), 7.72 (d, 2H, dmbpy), 8.30 (s, 2H, dmbpy), 8.81 (d, 2H, dmbpy). ^{13}C NMR (600 MHz, D_2O), $\delta = 23.60$ (dmbpy), 30.96 (pen), 34.57 (pen), 55.65 (pen), 75.48 (pen), 127.31 (dmbpy), 131.16 (dmbpy), 150.52 (dmbpy), 157.89 (dmbpy), 158.61 (dmbpy), 183.66 (pen). UV-Vis spectrum in H_2O [ν_{max}, $10^3\,cm^{-1}$ (log ε/mol^{-1} dm^3 cm^{-1})]: 15.92 (1.84), 19.2 (2.2)^{sh}, 22.6 (2.8)^{sh}, 29.0 (3.8)^{sh}, 31.6 (4.2)^{sh}, 32.8 (4.2)^{sh}, 34.84 (4.28), 42.19 (4.66). CD spectrum in H_2O [ν_{max}, $10^3\,cm^{-1}$ ($\Delta\varepsilon$)]: 15.86 (−2.54), 19.42 (+9.63), 22.8 (−8.6)^{sh}, 25.32 (−17.05), 28.09 (−16.83), 32.36 (+41.51), 35.6 (+34.7), 39.8 (+29.2)^{sh}, 42.19 (+41.39). Diffuse reflectance spectrum [ν_{max}, $10^3\,cm^{-1}$]: 15.62, 19.1^{sh}, 21.9^{sh}, 28.25, 31.20, 32.3^{sh}, 34.0^{sh}, 40.32.

2.5. *Preparation of [Pd(dmbpy){Co(L-pen)$_2$}]Cl • 3H$_2$O (2bCl • 3H$_2$O)*

This complex was prepared by a similar method to that for **2a**Cl · 3H_2O, using K[Co(L-pen)$_2$] · 2.5H_2O instead of K[Co(D-pen)$_2$] · 2.5H_2O. Yield: 0.25 g (68% based on Co). Anal. Calcd for $C_{22}H_{36}N_4O_7S_2ClCoPd$ (**2b**Cl · 3H_2O): C, 36.02; H, 4.95; N, 7.64%. Found: C, 36.03; H, 4.99; N, 7.57%. ^{1}H NMR (600 MHz, D_2O), $\delta = 1.59$ (s, 6H, pen), 1.90 (s, 6H, pen), 2.65 (s, 6H, dmbpy), 3.85 (s, 2H, pen), 7.71 (d, 2H, dmbpy), 8.30 (s, 2H, dmbpy), 8.81 (d, 2H, dmbpy). ^{13}C NMR (600 MHz, D_2O), $\delta = 23.61$ (dmbpy), 30.97 (pen), 34.57 (pen), 55.64 (pen), 75.48 (pen), 127.32 (dmbpy), 131.17 (dmbpy), 150.54 (dmbpy), 157.86 (dmbpy), 158.64 (dmbpy), 183.72 (pen). UV-Vis spectrum in H_2O [ν_{max}, $10^3\,cm^{-1}$ (log ε/mol^{-1} dm^3 cm^{-1})]: 15.90 (1.83), 19.2 (2.1)^{sh}, 22.6 (2.8)^{sh}, 29.1 (3.8)^{sh}, 31.6 (4.2)^{sh}, 32.7 (4.2)^{sh}, 34.72 (4.20), 42.13 (4.63). CD spectrum in H_2O [ν_{max}, $10^3\,cm^{-1}$ ($\Delta\varepsilon$)]: 15.90 (+2.42), 19.46 (−8.96), 22.8 (+7.9)^{sh}, 25.38 (+15.82), 28.09 (+15.33), 32.47 (−39.62), 35.5 (−34.4)^{sh}, 39.7 (−27.3)^{sh}, 42.01 (−38.56). Diffuse reflectance spectrum [ν_{max}, $10^3\,cm^{-1}$]: 15.77, 19.0^{sh}, 21.9^{sh}, 28.17, 31.15, 32.3^{sh}, 34.0^{sh}, 40.24.

2.6. *Preparation of [Pd(dmbpy){Co(D-pen)$_2$}]$_{0.5}$[Pd(dmbpy){Co(L-pen)$_2$}]$_{0.5}$Cl • 7H$_2$O (2cCl • 7H$_2$O)*

To a brown solution containing **2a**Cl · 3H_2O (0.18 g, 0.25 mmol) in 10 mL H_2O was added **2b**Cl · 3H_2O (0.18 g, 0.25 mmol) in 10 mL H_2O. After the mixture was allowed to stand at 25°C for several days, the resulting brown crystals were collected by filtration. Yield: 0.34 g (84% based on Co). Anal. Calcd for $C_{22}H_{44}N_4O_{11}S_2ClCoPd$ (**2c**Cl · 7H_2O): C, 32.80; H, 5.50; N, 6.96%. Found: C, 32.77; H, 5.51; N, 6.90%. ^{1}H NMR (600 MHz, D_2O), $\delta = 1.56$ (s, 6H, pen), 1.87 (s, 6H, pen), 2.63 (s, 6H, dmbpy), 3.82 (s, 2H, pen), 7.68 (d, 2H, dmbpy), 8.28 (s, 2H, dmbpy), 8.79 (d, 2H, dmbpy). ^{13}C NMR (600 MHz, D_2O), $\delta = 23.59$ (dmbpy), 30.96 (pen), 34.53 (pen), 55.63 (pen), 75.48 (pen), 127.32 (dmbpy), 131.14 (dmbpy), 150.54 (dmbpy), 157.86 (dmbpy), 158.71 (dmbpy), 183.75 (pen). UV-Vis spectrum in H_2O [ν_{max}, $10^3\,cm^{-1}$ (log ε/mol^{-1} dm^3 cm^{-1})]: 15.85 (1.90), 19.2 (2.1)^{sh}, 22.6 (2.8)^{sh}, 29.0 (3.9)^{sh}, 31.6 (4.2)^{sh}, 32.7 (4.3)^{sh}, 34.84 (4.35), 42.19 (4.77). Diffuse reflectance spectrum [ν_{max}, $10^3\,cm^{-1}$]: 15.62, 21.2^{sh}, 28.22, 31.05, 32.2^{sh}, 34.1^{sh}, 39.2^{sh}.

2.7. *Preparation of [Pt(dmbpy){Co(D-pen)$_2$}]Cl • 3H$_2$O (3aCl • 3H$_2$O)*

This complex was prepared by a similar method to that for **2a**Cl · 3H$_2$O, using [PtCl$_2$(dmbpy)] instead of [PdCl$_2$(dmbpy)]. Yield: 0.31 g (75% based on Co). Anal. Calcd for $C_{22}H_{36}N_4O_7S_2ClCoPt$ (**3a**Cl · 3H$_2$O): C, 32.14; H, 4.41; N, 6.81%. Found: C, 32.16; H, 4.41; N, 6.76%. ^{1}H NMR (600 MHz, D$_2$O), $\delta = 1.57$ (s, 6H, pen), 1.77 (s, 6H, pen), 2.66 (s, 6H, dmbpy), 4.00 (s, 2H, pen), 7.77 (d, 2H, dmbpy), 8.34 (s, 2H, dmbpy), 8.96 (d, 2H, dmbpy). ^{13}C NMR (600 MHz, D$_2$O), $\delta = 23.78$ (dmbpy), 31.05 (pen), 34.60 (pen), 54.60 (pen), 75.86 (pen), 127.58 (dmbpy), 131.60 (dmbpy), 149.30 (dmbpy), 158.23 (dmbpy), 158.94 (dmbpy), 183.62 (pen). UV-Vis spectrum in H$_2$O [ν_{max}, 10^3 cm^{-1} (log ε/mol^{-1} dm^3 cm^{-1})]: 16.23 (2.05), 19.30 (2.07), 25.0 (3.2)^{sh}, 29.0 (3.8)^{sh}, 31.45 (4.32), 32.68 (4.29), 37.9 (4.3)^{sh}, 41.3 (4.5)^{sh}, 47.85 (4.67). CD spectrum in H$_2$O [ν_{max}, 10^3 cm^{-1} ($\Delta\varepsilon$)]: 16.16 (−5.00), 19.42 (+8.08), 22.1 (+0.7)^{sh}, 25.44 (−6.00), 28.4 (+11.2)^{sh}, 29.85 (+15.58), 31.15 (+15.90), 38.17 (+26.93), 44.23 (+33.89). Diffuse reflectance spectrum [ν_{max}, 10^3 cm^{-1}]: 16.01, 19.29, 25.2^{sh}, 28.2^{sh}, 31.00, 32.2^{sh}, 40.1^{sh}.

2.8. *Preparation of [Pt(dmbpy){Co(L-pen)$_2$}]Cl • 3H$_2$O (3bCl • 3H$_2$O)*

This complex was prepared by a similar method to that for **3a**Cl · 3H$_2$O, using K[Co(L-pen)$_2$] · 2.5H$_2$O instead of K[Co(D-pen)$_2$] · 2.5H$_2$O. Yield: 0.32 g (78% based on Co). Anal. Calcd for $C_{22}H_{36}N_4O_7S_2ClCoPt$ (**3b**Cl · 3H$_2$O): C, 32.14; H, 4.41; N, 6.81%. Found: C, 32.12; H, 4.45; N, 6.78%. ^{1}H NMR (600 MHz, D$_2$O), $\delta = 1.57$ (s, 6H, pen), 1.77 (s, 6H, pen), 2.66 (s, 6H, dmbpy), 4.00 (s, 2H, pen), 7.78 (d, 2H, dmbpy), 8.34 (s, 2H, dmbpy), 8.96 (d, 2H, dmbpy). ^{13}C NMR (600 MHz, D$_2$O), $\delta = 23.78$ (dmbpy), 31.05 (pen), 34.60 (pen), 54.60 (pen), 75.85 (pen), 127.58 (dmbpy), 131.59 (dmbpy), 149.30 (dmbpy), 158.22 (dmbpy), 158.95 (dmbpy), 183.64 (pen). UV-Vis spectrum in H$_2$O [ν_{max}, 10^3 cm^{-1} (log ε/mol^{-1} dm^3 cm^{-1})]: 16.23 (2.05), 19.42 (2.06), 25.0 (3.2)^{sh}, 29.0 (3.8)^{sh}, 31.45 (4.32), 32.68 (4.29), 37.9 (4.3)^{sh}, 41.2 (4.5)^{sh}, 47.62 (4.67). CD spectrum in H$_2$O [ν_{max}, 10^3 cm^{-1} ($\Delta\varepsilon$)]: 16.08 (+4.98), 19.42 (−8.06), 22.1 (−0.7)^{sh}, 25.44 (+5.97), 28.4 (−10.8)^{sh}, 29.85 (−14.94), 31.15 (−15.20), 38.02 (−25.87), 44.44 (−32.63). Diffuse reflectance spectrum [ν_{max}, 10^3 cm^{-1}]: 16.03, 19.21, 25.2^{sh}, 28.2^{sh}, 31.00, 32.2^{sh}, 40.2^{sh}.

2.9. *Preparation of [Pt(dmbpy){Co(D-pen)$_2$}]$_{0.5}$[Pt(dmbpy){Co(L-pen)$_2$}]$_{0.5}$Cl • 6H$_2$O (3cCl • 6H$_2$O)*

To a dark green solution containing **3a**Cl · 3H$_2$O (0.20 g, 0.25 mmol) in 10 mL H$_2$O was added **3b**Cl · 3H$_2$O (0.20 g, 0.25 mmol) in 10 mL H$_2$O. After the mixture was allowed to stand at 25°C for several days, the resulting green crystals were collected by filtration. Yield: 0.35 g (80% based on Co). Anal. Calcd for $C_{22}H_{42}N_4O_{10}S_2ClCoPt$ (**3c**Cl · 6H$_2$O): C, 30.16; H, 4.83; N, 6.39%. Found: C, 30.18; H, 4.79; N, 6.32%. ^{1}H NMR (600 MHz, D$_2$O), $\delta = 1.54$ (s, 6H, pen), 1.74 (s, 6H, pen), 2.63 (s, 6H, dmbpy), 3.96 (s, 2H, pen), 7.73 (d, 2H, dmbpy), 8.30 (s, 2H, dmbpy), 8.93 (d, 2H, dmbpy). ^{13}C NMR (600 MHz, D$_2$O), $\delta = 23.77$ (dmbpy), 31.04 (pen), 34.56 (pen), 54.58 (pen), 75.85 (pen), 127.57 (dmbpy), 131.57 (dmbpy), 149.30 (dmbpy), 158.20 (dmbpy), 158.99 (dmbpy), 183.65 (pen). UV-Vis spectrum in H$_2$O [ν_{max}, 10^3 cm^{-1} (log ε/mol^{-1} dm^3 cm^{-1})]: 16.18 (2.08), 19.34 (2.09), 25.0 (3.3)^{sh}, 29.1 (3.8)^{sh}, 31.45 (4.36), 32.68 (4.33), 37.9 (4.4)^{sh}, 41.2 (4.5)^{sh}, 48.08 (4.70). Diffuse reflectance spectrum [$\nu_{\max}$, $10^3\,\mathrm{cm}^{-1}$]: 16.01, 19.32, 27.99, 30.69, 31.9^{sh}, 40.2^{sh}.

2.10. *Measurements*

Electronic absorption spectra were recorded with a Perkin-Elmer Lambda 19 spectrophotometer, and the CD spectra with a JASCO J-600 spectropolarimeter. These measurements were carried out in aqueous solutions at room temperature. Diffuse reflectance spectra were measured with a JASCO Ubest V-570 spectrophotometer equipped with an integrating sphere apparatus. ^{1}H and ^{13}C NMR spectra were recorded with a Bruker AVANCE-600 NMR spectrometer in D_2O, using sodium 4,4-dimethyl-4-silapentane-1-sulfonate (DSS) as an internal reference. Elemental analyses (C, H, N) were performed with a Perkin-Elmer 2400 CHN Elemental Analyzer.

2.11. *X-ray structure determination*

Single crystals of **1b**Cl · $3H_2O$, **1c**Cl · $7H_2O$, **2c**Cl · $7H_2O$, and **3c**Cl · $6H_2O$ were used for data collection on a Rigaku AFC5S automated four-circle diffractometer with graphite-monochromatized Mo-Kα ($\lambda = 0.71069$ Å) radiation. Cell constants and an orientation matrix for data collection were obtained from a least-squares refinement using the setting angles of 25 carefully centered reflections in the range $14° < \theta < 15°$ for **1b**Cl · $3H_2O$, **1c**Cl · $7H_2O$, **2c**Cl · $7H_2O$, and **3c**Cl · $6H_2O$. The data were collected at a temperature of 296 ± 1 K using the ω-2θ scan technique to a maximum 2θ value of 55°. The weak reflections ($I < 10.0\sigma(I)$) were rescanned (maximum of 3 scans) and the counts were accumulated to ensure good counting statistics. Stationary background counts were recorded on each side of the reflection. The ratio of peak counting time to background counting time was 2 : 1. The intensities of three representative reflections were measured after every 150 reflections. Over the course of data collection, the standards decreased by 0.2–8.6%. Polynomial correction factors were applied to the data to account for this phenomenon. Empirical absorption corrections based on azimuthal scans of several reflections were applied. The data were corrected for Lorentz and polarization effects. Corrections for secondary extinctions were applied for **1c**Cl · $7H_2O$, **2c**Cl · $7H_2O$, and **3c**Cl · $6H_2O$ [10]. The crystal data and experimental parameters are summarized in table 1.

The structures were solved by direct methods for **1b**Cl · $3H_2O$, **1c**Cl · $7H_2O$, **2c**Cl · $7H_2O$, and **3c**Cl · $6H_2O$, and expanded using Fourier techniques [11, 12]. The non-hydrogen atoms were refined anisotropically. All the hydrogen atoms were refined using the riding model. The final cycle of full-matrix least-squares refinement on *F* was based on observed reflections ($I > 2.00\sigma(I)$) and variable parameters, and converged with unweighted and weighted agreement factors of *R* and *Rw*. Neutral atom scattering factors were taken from Cromer and Waber [13]. Anomalous dispersion effects were included in *Fc*; the values for $\Delta f'$ and $\Delta f'$ were those of Creagh and McAuley [14–16]. The absolute configuration for **1b**Cl · $3H_2O$ was determined on the basis of the known *R* configurations of the asymmetric carbon atoms in the L-pen ligands, and the structure was supported by the Flack parameter of $-0.1(1)$ [17]. All calculations were performed

Table 1. Crystallographic data for **1b**Cl · $3H_2O$, **1c**Cl · $7H_2O$, **2c**Cl · $7H_2O$, and **3c**Cl · $6H_2O$.

	1bCl · $3H_2O$	**1c**Cl · $7H_2O$	**2c**Cl · $7H_2O$	**3c**Cl · $6H_2O$
Formula	$C_{20}H_{32}N_4O_7$ $S_2ClCoPd$	$C_{20}H_{40}N_4O_{11}$ $S_2ClCoPd$	$C_{22}H_{44}N_4O_{11}$ $S_2ClCoPd$	$C_{22}H_{42}N_4O_{10}$ $S_2ClCoPt$
Formula weight	705.40	777.46	805.52	876.19
Crystal size (mm^3)	0.50 × 0.50 × 0.50	0.30 × 0.40 × 0.50	0.20 × 0.30 × 0.60	0.20 × 0.40 × 0.50
Space group	$P6_4$	$Pca2_1$	$P2_1/a$	$P2_1/a$
a (Å)	14.470(1)	8.537(4)	8.680(2)	8.691(4)
b (Å)		16.035(6)	16.961(2)	16.888(5)
c (Å)	11.816(1)	22.310(3)	22.797(1)	22.818(3)
α (°)				
β (°)			99.78(1)	99.74(2)
γ (°)				
V ($Å^3$)	2142.6(3)	3053(1)	3307.3(8)	3300(1)
Z	3	4	4	4
Dc ($g\,cm^{-3}$)	1.640	1.691	1.618	1.763
$\mu\,cm^{-1}$)	14.94	14.15	13.10	49.80
Trans. factors	0.93–1.00	0.89–0.98	0.90–0.99	0.72–1.00
Tot. reflections	1934	3962	8364	8347
Refl. $I > 2\sigma(I)$	1589	3042	5291	5818
No. of variables	183	389	410	401
R (R_w)	0.041 (0.056)	0.046 (0.066)	0.064 (0.105)	0.054 (0.086)
Goodness-of fit on F^2	1.00	1.01	1.00	1.00

using the CrystalStructure crystallographic software package of Molecular Structure Corporation [18].

3. Results and discussion

3.1. *Crystal structures*

An X-ray structural analysis for **1b**Cl · $3H_2O$ revealed the presence of a discrete monovalent complex cation, one chloride anion, and three water molecules. Perspective drawing of the complex cation **1b** is given in figure 1, and selected bond distances and angles are listed in table 2. As shown in figure 1, **1b** is composed of one Co atom and one Pd atom to form an S-bridged dinuclear structure. The Co atom in **1b** is surrounded by two N, O, and S atoms from two L-pen ligands, retaining the *trans*(*N*) geometry of the octahedral Co(III) unit as the starting material, namely, equatorial coordination sites of the Co atom are occupied by two O and S atoms, and axial ones by two N atoms to adopt an octahedral *trans*(*N*)-$[Co(L\text{-}pen)_2]^-$ unit. The Pd atom in **1b** is coordinated by two N atoms from bpy and bridged by two S atoms from the *trans*(N)-$[Co(L\text{-}pen)_2]^-$ unit to acquire a square-planar geometry. The Co(III) equatorial plane and PdS_2N_2 plane in **1b** are almost coplanar (dihedral angle: 1.2°), and the Pd atom in **1b** acquires an almost square-planar geometry (dihedral angle between the Pd1S1S1* and PdN2N2* planes: 0.5°). These structural features for **1b** are consistent with those for **1a**, except for absolute configurations of asymmetric carbon in penicillaminates [3]. In fact, the bond distances and angles around the Co(III) and Pd(II) atoms in **1a** are almost identical with

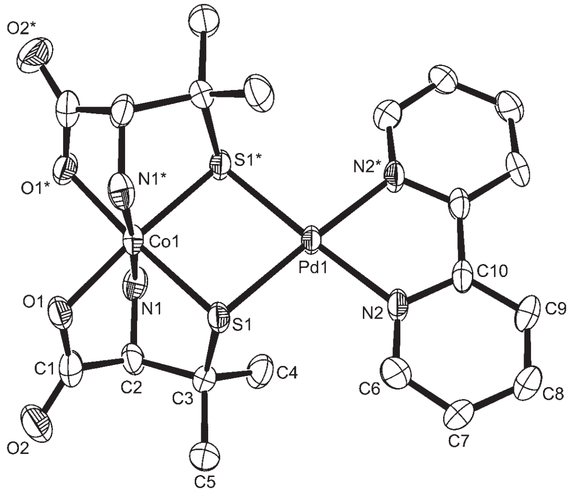

Figure 1. Perspective view of **1b** with the atomic labeling scheme (50% probability ellipsoids). Symmetry codes for the atoms with asterisks: $1-x$, $-y$, z.

Table 2. Selected bond distances (Å) and angles (deg) for **1b**Cl · 3H$_2$O and **1c**Cl · 7H$_2$O.

1bCl · 3H$_2$O		**1c**Cl · 7H$_2$O	
Pd(1)–S(1)	2.295(3)	Pd(1)–S(1)	2.311(2)
Pd(1)–S(1)*	2.295(3)	Pd(1)–S(2)	2.292(3)
Pd(1)–N(2)	2.048(8)	Pd(1)–N(3)	2.072(8)
Pd(1)–N(2)*	2.048(8)	Pd(1)–N(4)	2.095(8)
Co(1)–S(1)	2.221(4)	Co(1)–S(1)	2.225(3)
Co(1)–S(1)*	2.221(4)	Co(1)–S(2)	2.228(3)
Co(1)–O(1)	1.929(8)	Co(1)–O(1)	1.958(7)
Co(1)–O(1)*	1.929(8)	Co(1)–O(3)	1.951(7)
Co(1)–N(1)	1.943(7)	Co(1)–N(1)	1.938(8)
Co(1)–N(1)*	1.943(7)	Co(1)–N(2)	1.928(8)
Pd(1)–S(1)–Co(1)	94.8(1)	Pd(1)–S(1)–Co(1)	95.2(1)
S(1)*–Pd(1)–S(1)	83.5(1)	S(2)–Pd(1)–S(1)	82.88(8)
N(2)–Pd(1)–S(1)	98.8(2)	N(3)–Pd(1)–S(1)	100.2(2)
N(2)*–Pd(1)–S(1)	177.6(3)	N(4)–Pd(1)–S(1)	176.3(2)
Pd(1)–S(1)*–Co(1)	94.8(1)	Pd(1)–S(2)–Co(1)	95.6(1)
N(2)–Pd(1)–S(1)*	177.6(3)	N(3)–Pd(1)–S(2)	176.7(2)
N(2)*–Pd(1)–S(1)*	98.8(2)	N(4)–Pd(1)–S(2)	97.8(2)
N(2)*–Pd(1)–N(2)	78.9(3)	N(4)–Pd(1)–N(3)	79.3(3)
S(1)*–Co(1)–S(1)	86.9(2)	S(2) Co(1)–S(1)	86.31(9)
O(1)–Co(1)–S(1)	89.5(2)	O(1)–Co(1)–S(1)	92.0(2)
O(1)*–Co(1)–S(1)	175.6(3)	O(3)–Co(1)–S(1)	175.2(2)
N(1)–Co(1)–S(1)	88.3(2)	N(1)–Co(1)–S(1)	88.4(3)
N(1)*–Co(1)–S(1)	95.4(2)	N(2)–Co(1)–S(1)	96.1(2)
O(1)–Co(1)–S(1)*	175.6(3)	O(1)–Co(1)–S(2)	177.9(3)
O(1)*–Co(1)–S(1)*	89.5(2)	O(3)–Co(1)–S(2)	89.2(2)
N(1)–Co(1)–S(1)*	95.4(2)	N(1)–Co(1)–S(2)	96.6(2)
N(1)*–Co(1)–S(1)*	88.3(2)	N(2)–Co(1)–S(2)	89.0(3)
O(1)*–Co(1)–O(1)	94.1(3)	O(3)–Co(1)–O(1)	92.5(3)
N(1)–Co(1)–O(1)	81.9(3)	N(1)–Co(1)–O(1)	82.0(3)
N(1)*–Co(1)–O(1)	94.6(3)	N(2)–Co(1)–O(1)	92.5(3)
N(1)–Co(1)–O(1)*	94.6(3)	N(1)–Co(1)–O(3)	93.8(3)
N(1)*–Co(1)–O(1)*	81.9(3)	N(2)–Co(1)–O(3)	82.1(3)
N(1)*–Co(1)–N(1)	175.0(4)	N(2)–Co(1)–N(1)	173.0(3)

*Symmetry codes for the atoms with asterisks: $1-x$, $-y$.

those in **1b**. Although two chiral configurations, *R* and *S*, are possible for each of the two bridging S atoms in **1b**, both S atoms are stereoselectively unified to the *R* configurations in contrast to the S atoms with *S* configurations in the *trans*(*N*)-$[Co(\text{D-pen})_2]^-$ unit of **1a**. The optically active complex cation **1b** exists as a monomer, accompanied by no intermolecular interactions in the π-electronic systems of the bpy moieties. This is a marked difference from the other S-bridged dinuclear complexes with square-planar $[M(II)(\mu\text{-}S)_2(bpy)]$ frameworks, but is consistent with the optically active $[M(bpy)\{Co(\text{D-pen})_2\}]^+$, $[Pt(bpy)\{Co(\text{L-pen})_2\}]^+$, Δ-$[M(bpy)\{Co(aet)_2(R\text{-pn})\}]^{3+}$, and Λ-$[Pt(bpy)\{Co(aet)_2(S\text{-pn})\}]^{3+}$ [2–5].

The mixture of equimolar amounts of **1a**$Cl \cdot 3H_2O$ and **1b**$Cl \cdot 3H_2O$ in H_2O crystallizes as **1c**$Cl \cdot 7H_2O$ in the orthorhombic space group of $Pca2_1$, in remarkable contrast with the hexagonal space group of $P6_2$ for **1a**$Cl \cdot 3H_2O$ or $P6_4$ **1b**$Cl \cdot 3H_2O$ (table 1) [3]. Although the enantiomeric complex cations **1a** and **1b** are included at a ratio of 1 : 1 in the crystals of **1c**$Cl \cdot 7H_2O$, only one monovalent complex cation is a crystallographically independent. As shown in table 2, there are no significant distinctions in the bond distances and angles around the Co(III) and Pd(II) atoms between **1c** and **1b** (or **1a**) [3]. However, the Co(III) equatorial plane and PdS_2N_2 plane in **1c** are somewhat bent in comparison with **1b** (dihedral angle for **1c**: 1.9°). Furthermore, the dihedral angle between PdS_2 and PtN_2 planes in **1c** is 4.2°, which is eight times as large as the corresponding angle in **1b**, indicating less planarity of the PdS_2N_2 coordination sphere in **1c**. These facts suggest intermolecular interactions exist in the crystals of **1c**$Cl \cdot 7H_2O$. As shown in figure 2, the enantiomeric complex cations, $[Pd(bpy)\{Co(\text{D-pen})_2\}]^+$ and $[Pd(bpy)\{Co(\text{L-pen})_2\}]^+$, are arranged alternately with

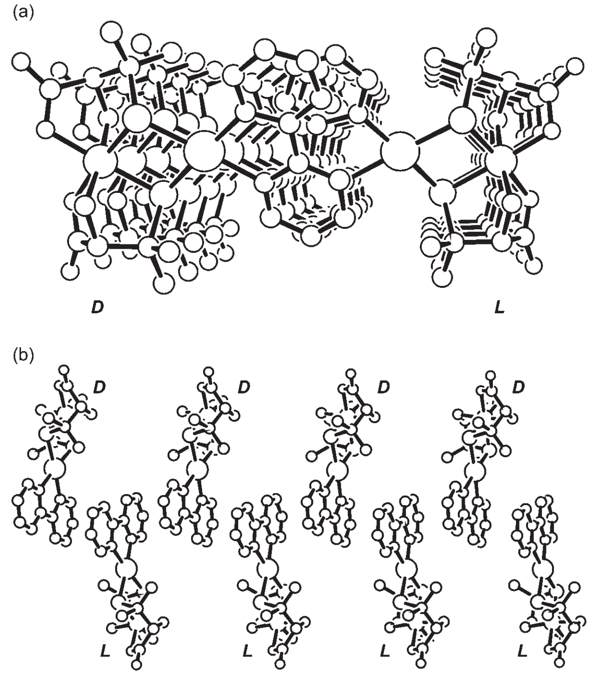

Figure 2. Projection for the linear-chain comprised of enantiomeric complex cations, $[Pd(bpy)\{Co(\text{D-pen})_2\}]^+$ (***D***) and $[Pd(bpy)\{Co(\text{D-pen})_2\}]^+$ (***L***), in **1c**$Cl \cdot 7H_2O$ (a) viewed along *a* axis and (b) *c* axis.

overlapping bpy planes along the *a* axis. Additionally, the distance of the bpy plane in $[Pd(bpy)\{Co(\text{L-pen})_2\}]^+$ from one adjacent bpy plane in $[Pd(bpy)\{Co(\text{D-pen})_2\}]^+$ is 3.45 Å, and that from another adjacent bpy plane in $[Pd(bpy)\{Co(\text{D-pen})_2\}]^+$ is 3.54 Å. These two interaction modes with different interplane distances result in the formation of a polymeric π–π stacking chain. Such structural characteristics are consistent with those observed for $[Pt(bpy)\{Co(\text{D-pen})_2\}]_{0.5}[Pt(bpy)\{Co(\text{L-pen})_2\}]_{0.5}Cl \cdot 7H_2O$ [4].

In contrast with the acentric space group $Pca2_1$ of **1c**$Cl \cdot 7H_2O$, the mixture of equimolar amounts of **2a**$Cl \cdot 3H_2O$ and **2b**$Cl \cdot 3H_2O$ in H_2O crystallizes as **2c**$Cl \cdot 7H_2O$ in the centric space group $P2_1/a$ (table 1). In common with **1c**$Cl \cdot 7H_2O$, only one monovalent complex cation is crystallographically independent in **2c**$Cl \cdot 7H_2O$, while the enantiomeric complex cations **2a** and **2b** are included by the ratio of 1 : 1 in the crystals. In **2c**$Cl \cdot 7H_2O$, furthermore, the enantiomeric complex cations, $[Pd(dmbpy)\{Co(\text{D-pen})_2\}]^+$ and $[Pd(dmbpy)\{Co(\text{L-pen})_2\}]^+$, are arranged alternately while overlapping the dmbpy planes to form a polymeric π–π stacking chain. Similarly to **2c**$Cl \cdot 7H_2O$, the aqueous solution mixture of **3a**$Cl \cdot 3H_2O$ and **3b**$Cl \cdot 3H_2O$ crystallizes as **3c**$Cl \cdot 6H_2O$ in the centric space group $P2_1/a$, and the crystals of **2c**$Cl \cdot 7H_2O$ and **3c**$Cl \cdot 6H_2O$ are almost isostructural (table 3). In **3c**$Cl \cdot 6H_2O$, the π–π stacking chain is also developed by alternately arranged enantiomeric complex cations,

Table 3. Selected bond distances (Å) and angles (deg) of **2c**$Cl \cdot 7H_2O$ (M = Pd) and **3c**$Cl \cdot 6H_2O$ (M = Pt).

	2c$Cl \cdot 7H_2O$	**3c**$Cl \cdot 6H_2O$
M(1)–S(1)	2.297(2)	2.301(3)
M(1)–S(2)	2.302(2)	2.292(3)
M(1)–N(3)	2.057(7)	2.05(1)
M(1)–N(4)	2.061(7)	2.042(9)
Co(1)–S(1)	2.222(2)	2.217(3)
Co(1)–S(2)	2.215(2)	2.220(3)
Co(1)–O(1)	1.948(6)	1.949(7)
Co(1)–O(3)	1.935(6)	1.939(8)
Co(1)–N(1)	1.932(6)	1.943(8)
Co(1)–N(2)	1.939(6)	1.946(8)
M(1)–S(1)–Co(1)	94.78(9)	95.0(1)
S(2)–M(1)–S(1)	83.27(7)	83.08(9)
N(3)–M(1)–S(1)	98.7(2)	99.1(3)
N(4)–M(1)–S(1)	176.9(2)	178.5(3)
M(1)–S(2)–Co(1)	94.83(8)	95.1(1)
N(3)–M(1)–S(2)	177.6(2)	176.7(3)
N(4)–M(1)–S(2)	98.7(2)	97.9(3)
N(4)–M(1)–N(3)	79.4(3)	79.9(4)
S(2)–Co(1)–S(1)	87.03(8)	86.7(1)
O(1)–Co(1)–S(1)	89.1(2)	91.5(3)
O(3)–Co(1)–S(1)	178.0(2)	175.5(2)
N(1)–Co(1)–S(1)	88.1(2)	87.9(3)
N(2)–Co(1)–S(1)	94.8(2)	95.2(3)
O(1)–Co(1)–S(2)	175.6(2)	177.5(2)
O(3)–Co(1)–S(2)	91.5(2)	89.2(2)
N(1)–Co(1)–S(2)	95.5(2)	95.5(3)
N(2)–Co(1)–S(2)	88.2(2)	87.8(3)
O(3)–Co(1)–O(1)	92.4(2)	92.7(3)
N(1)–Co(1)–O(1)	82.2(3)	82.7(3)
N(2)–Co(1)–O(1)	94.3(3)	94.0(3)
N(1)–Co(1)–O(3)	93.5(3)	94.3(3)
N(2)–Co(1)–O(3)	83.7(3)	82.8(3)
N(2)–Co(1)–N(1)	175.5(3)	175.5(4)

[Pt(dmbpy){Co(D-pen)$_2$}]$^+$ and [Pt(dmbpy){Co(L-pen)$_2$}]$^+$. The distance between the dmbpy planes in **2c**Cl · 7H_2O is 3.59 Å, and that in **3c**Cl · 6H_2O is 3.60 Å. Although these interplane distances between the dmbpy planes are considerably longer than the corresponding ones in **1c**Cl · 7H_2O, interactions between the π electronic systems in the dmbpy frameworks of the enantiomeric units in **2c**Cl · 7H_2O and **3c**Cl · 6H_2O are indicated.

3.2. *Characterization*

In D_2O, ^{13}C NMR spectrum of **1b** shows five signals due to the L-pen ligands and five signals characteristic for the coordinated bpy ligand [1–5, 19–21]. The other monomeric optically active dinuclear complex cations, **2a**, **2b**, **3a**, and **3b**, exhibit similar ten signals due to the bpy and pen ligands, accompanied by additional signals ascribed as the carbon atoms of –CH_3 groups in the dmbpy ligands. Although two kinds of complex cations, [Pd(bpy){Co(D-pen)$_2$}]$^+$ and [Pd(bpy){Co(L-pen)$_2$}]$^+$, exist in **1c**Cl · 7H_2O, on the other hand, the ^{13}C NMR spectrum exhibits five signals due to the pen ligands and five signals characteristic for the bpy ligand. Furthermore, the pattern of **1c**Cl · 7H_2O in D_2O is quite similar to those of **1a** and **1b**. A similar trend is also observed for ^{1}H NMR spectra of **1a**, **1b**, and **1c** [3]. Similarly, the NMR spectral behaviors of **2c** and **3c**, which take dimeric structures in the crystalline state, are almost identically with those of **2a** (or **2b**) and **3a** (or **3b**), respectively. These facts indicate no intermolecular interactions at concentrations of 10^{-2} mol dm^{-3}. It seems therefore that each enantiomeric complex cation in **1c**Cl · 7H_2O, **2c**Cl · 7H_2O, or **3c**Cl · 6H_2O exists as a monomer in solution as well as **1a**Cl · 3H_2O, **1b**Cl · 3H_2O, **2a**Cl · 3H_2O, **2b**Cl · 3H_2O, **3a**Cl · 3H_2O, or **3b**Cl · 3H_2O.

Electronic absorption and CD spectra of **1b**Cl · 3H_2O, **2b**Cl · 3H_2O, and **3b**Cl · 3H_2O, which exist as monomers in the crystalline state, in H_2O are shown in figure 3. The first absorption band of **1b** is comprised of three components at 15.82, 19.1, and 22.6×10^3 cm^{-1}. In addition, **1b** shows a second d–d and sulfur-to-metal charge-transfer band at 29.2 and 34.96×10^3 cm^{-1}, respectively [3]. Furthermore, the characteristic bands due to the localized electronic transitions on the bpy framework appear at 31.2 and 32.36×10^3 cm^{-1} [1–5, 9, 19]. While the absorption spectral profile of **2b** is almost the same as that of **1b**, the localized electronic bands on the π framework in **2b** appear at higher energy than the corresponding bands in **1b**. A similar trend is also observed for the spectrum of **3b**, when compared to that of [Pt(bpy){Co(L-pen)$_2$}]$^+$ [4]. It can be concluded therefore, that such higher-energy shifts in **2b** and **3b** arise from the inductions of methyl groups into π electronic systems. Absorption spectral features of **1b**Cl · 3H_2O, **2b**Cl · 3H_2O, and **3b**Cl · 3H_2O are essentially consistent with those of **1a**Cl · 3H_2O, **2a**Cl · 3H_2O, and **3a**Cl · 3H_2O, respectively, reflecting the enantiomeric relationships between complexes [3]. Although **1c**Cl · 7H_2O, **2c**Cl · 7H_2O, and **3c**Cl · 6H_2O involve two enantiomeric components and take dimeric structures in the crystalline state, their spectral patterns are quite similar to monomeric **1a**Cl · 3H_2O (or **1b**Cl · 3H_2O), **2a**Cl · 3H_2O (or **2b**Cl · 3H_2O), **3a**Cl · 3H_2O (or **3b**Cl · 3H_2O), respectively. These results also seem to support no significant interaction between the π electronic systems **1c**Cl · 7H_2O, **2c**Cl · 7H_2O, and **3c**Cl · 6H_2O in H_2O. The CD spectrum of **1b** is comprised of four positive bands at 15.92, 22.9, 25.51, and 28.25×10^3 cm^{-1}, and five negative bands at 19.46, 32.25, 35.5, 40.2, and 43.10×10^3 cm^{-1}. While the

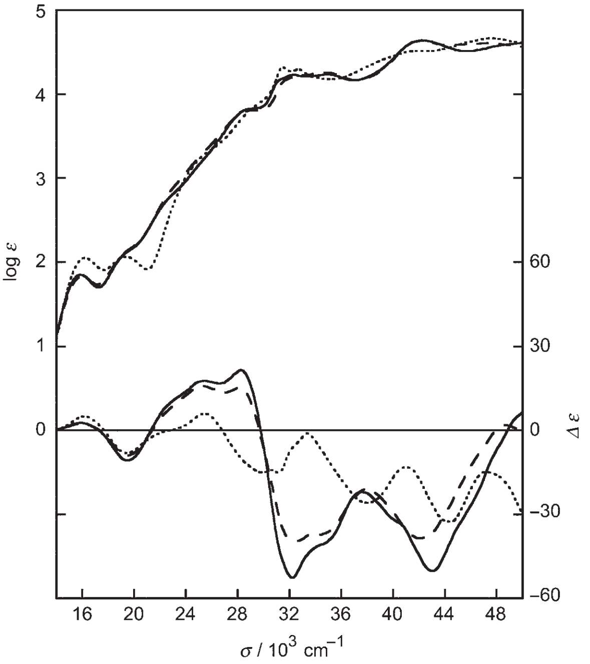

Figure 3. Electronic absorption and CD spectra of **1b**Cl · $3H_2O$ (solid line) **2b**Cl · $3H_2O$ (broken line), and **3b**Cl · $3H_2O$ (dotted line) in H_2O.

positions and absolute values of strengths of these CD bands correspond well with those for **1a**, the signs are opposite to the corresponding signs of **1a** on the basis of the enantiomeric relationship [3]. In contrast to the optically active **1a** and **1b**, **1c**Cl · $7H_2O$ in H_2O shows no CD signals over the whole region. It can be concluded therefore that **1c**Cl · $7H_2O$ involves accurately equimolecular amounts of **1a** and **1b**. Similar CD spectral behaviors are also observed for **2c**Cl · $7H_2O$ and **3c**Cl · $6H_2O$, indicating that these complexes include equimolar amounts of two enantiomeric complex cations.

Reflectance spectrum of monomeric **1b**Cl · $3H_2O$ consists of three peaks at 15.75, 30.58, and $40.0 \times 10^3\,\text{cm}^{-1}$, and five shoulders at 19.0, 22.4, 28.5, 31.7, and $34.1 \times 10^3\,\text{cm}^{-1}$ (figure 4). It is obvious that the 15.75, 19.0, 22.4, 28.5, 30.58, 31.7, 34.1, and $40.0 \times 10^3\,\text{cm}^{-1}$ reflectance bands correspond to the 15.82, 19.1, 22.6, 29.2, 31.2, 32.36, 34.96, and $42.19 \times 10^3\,\text{cm}^{-1}$ absorption bands in H_2O, respectively. While all the bands are slightly shifted toward lower energy than the corresponding absorption bands, the essential distinction is not found among both spectra. This implies that each cation in the solid state is comparatively put on a free environment as well as in solution. The reflectance spectrum of dimeric **1c**Cl · $7H_2O$ roughly corresponds to the absorption spectrum in H_2O, but some significant differences can be seen between the two spectra. It seems therefore, that each complex cation in **1c**Cl · $7H_2O$ is put under different environment in both states. Furthermore, the reflectance spectral pattern of **1c**Cl · $7H_2O$ is rather dissimilar to that of **1b**Cl · $3H_2O$, excluding the lower energy components of the first d–d absorption band. In the spectrum of **1c**Cl · $7H_2O$, for instance, the bands corresponding to the 30.58 and

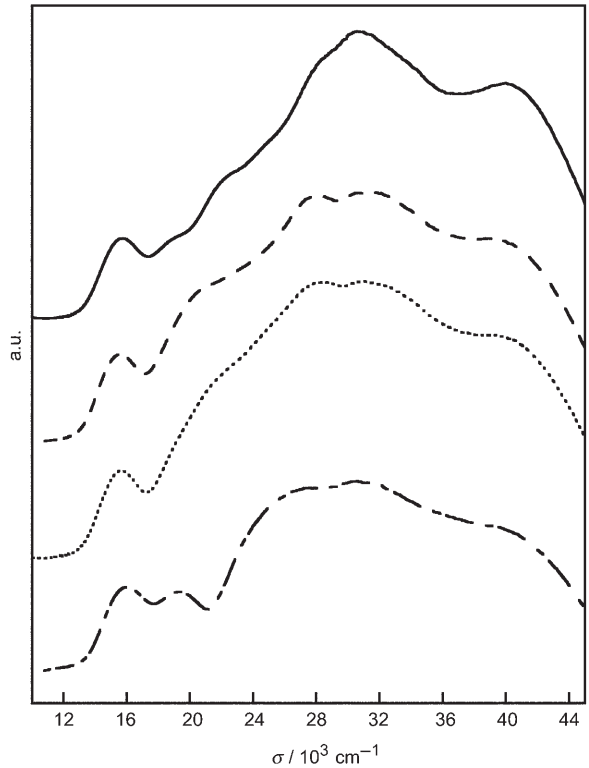

Figure 4. Diffuse reflectance spectra of **1b**Cl · $3H_2O$ (solid line), **1c**Cl · $7H_2O$ (broken line), **2c**Cl · $7H_2O$ (dotted line), and **3c**Cl · $7H_2O$ (dashed line).

$31.7 \times 10^3\,cm^{-1}$ bands of **1b**Cl · $3H_2O$ slightly shift toward lower energy at 30.4 and $31.6 \times 10^3\,cm^{-1}$. These two bands are assigned as localized electronic transitions on bpy, and hence the lower energy shift of **1c**Cl · $7H_2O$ is considered to be due to the π–π interactions between the bpy frameworks. A remarkable feature in the spectrum of **1c**Cl · $7H_2O$ is the emergence of the intense broad peak at $28.01 \times 10^3\,cm^{-1}$. Although the corresponding band is not found in the spectrum of **1b**Cl · $3H_2O$, similar bands are observed for the doubly S-bridged d^8 metal aromatic diimine complexes with intra- and/or intermolecular π–π stacking arrangements [19, 22, 23]. A similar reflectance band is also observed at $27.78 \times 10^3\,cm^{-1}$ for $[Pt(bpy)\{Co(\text{D-pen})_2\}]_{0.5}[Pt(bpy)\{Co(\text{L-pen})_2\}]_{0.5}Cl \cdot 7H_2O$, in which two enantiomers are arranged alternately while overlapping the bpy planes [4]. It can be regarded therefore, that the band at $28.01 \times 10^3\,cm^{-1}$ originates from formation of a polymeric π–π stacking chain between the enantiomeric complex cations in **1c**Cl · $7H_2O$. In dimeric **2c**Cl · $7H_2O$, the corresponding band to the $28.01 \times 10^3\,cm^{-1}$ band in **1c**Cl · $7H_2O$ locates at higher energy ($28.22 \times 10^3\,cm^{-1}$). Similarly, the characteristic band for π–π stacking in dimeric **3c**Cl · $6H_2O$ appears at higher energy ($27.99 \times 10^3\,cm^{-1}$) than $[Pt(bpy)\{Co(\text{D-pen})_2\}]_{0.5}[Pt(bpy)\{Co(\text{L-pen})_2\}]_{0.5}Cl \cdot 7H_2O$. These facts indicate that the band around $28 \times 10^3\,cm^{-1}$ in such complexes arise from the π frameworks.

Supplementary material

CCDC-644144 for **1b**$\cdot 3H_2O$, −644145 for **1c**Cl$\cdot 7H_2O$, −644146 for **2c**Cl$\cdot 7H_2O$, and −644147 for **3c**Cl$\cdot 7H_2O$, contain the supplementary crystallographic data for this article. These data can be obtained free of charge at www.ccdc.cam.ac.uk/conts/retrieving.html [or from the Cambridge Crystallographic Data Centre, 12, Union Road, Cambridge CB2 1EZ, UK; Fax: +44 1223 336 033; E-mail: deposit@ccdc.cam.ac.jk].

Acknowledgements

This work was partly supported by Grants-in-Aid for Scientific Research from the Ministry of Education, Culture, Sports, Science, and Technology.

References

[1] Y. Yamada, M. Uchida, Y. Miyashita, K. Fujisawa, T. Konno, K. Okamoto. *Bull. Chem. Soc. Jpn*, **73**, 913 (2000).

[2] Y. Yamada, Y. Maeda, T. Konno, K. Fujisawa, K. Okamoto. *Bull. Chem. Soc. Jpn*, **73**, 1831 (2000).

[3] Y. Yamada, M. Uchida, M. Fujita, Y. Miyashita, K. Okamoto. *Polyhedron*, **22**, 1507 (2003).

[4] Y. Yamada, K. Okamoto. *Inorg. Chim. Acta*, **359**, 3963 (2006).

[5] Y. Yamada, M. Noda, M. Inoue, Y. Miyashita, K. Okamoto, M. Koikawa, T. Tokii. *J. Coord. Chem.*, **60**, 607 (2007).

[6] K. Okamoto, K. Wakayama, H. Einaga, S. Yamada, J. Hidaka. *Bull. Chem. Soc. Jpn*, **56**, 165 (1983).

[7] N. Baidya, D. Ndreu, M. Olmstead, K. Mascharak. *Inorg. Chem.*, **30**, 2448 (1991).

[8] R.H. Herber, M. Croft, M.J. Coyer, B. Bilash, A. Sahiner. *Inorg. Chem.*, **33**, 2422 (1994).

[9] K. Okamoto, Y. Yoshinari, Y. Yamada, N. Sakagami, T. Konno. *Bull. Chem. Soc. Jpn*, **71**, 1363 (1998).

[10] A.C. Larson, F.R. Ahmed (Ed.). *Crystallographic Computing* (equation 22, with V replaced by the cell volume), Munksgaard, Copenhagen, pp. 291–294 (1970).

[11] *SIR92:A.* Altomare, G. Cascarano, C. Giacovazzo, A. Guagliardi, M. Burla, G. Polidori, M. Camalli. *J. Appl. Cryst.*, **27**, 435 (1994).

[12] P.T. Beurskens, G. Admiraal, G. Beurskens, W.P. Bosman, R. de Gelder, R. Israel, J.M.M. Smits. *DIRDIF99. The DIRDIF 99 program system*, Technical Report of the Crystallography Laboratory, University of Nijmegen, The Netherlands (1999).

[13] D.T. Cromer, J.T. Waber (Eds.). *International Tables for X-ray Crystallography*, Vol. IV, The Kynoch Press, Birmingham, England, Table 2.2 A (1974).

[14] J.A. Ibers, W.C. Hamilton. *Acta Cryst.*, **17**, 781 (1964).

[15] D.C. Creagh, W.J. McAuley. In *International Tables for Crystallography*, A.J.C. Wilson (Ed.), Vol. C, pp. 219–222, Kluwer Academic Publishers, Boston (1992).

[16] D.C. Creagh, J.H. Hubbell. In *International Tables for Crystallography*, A.J.C. Wilson (Ed.), Vol. C, pp. 200–206, Kluwer Academic Publishers, Boston (1992).

[17] H.D. Flack. *Acta Cryst.*, **A39**, 876 (1983).

[18] *Crystal Structure 3.6.0: Crystal Structure Analysis Package*, Rigaku and Rigaku/MSC, 9009 New Trails Dr. The Woodlands, TX 77381 USA (2004).

[19] Y. Yamada, K. Fujisawa, K. Okamoto. *Bull. Chem. Soc. Jpn*, **73**, 2067 (2000).

[20] Y. Yamada, M. Tsumita, A. Hirano, Y. Miyashita, K. Fujisawa, K. Okamoto. *Inorg. Chim. Acta*, **332**, 108 (2002).

[21] Y. Yamada, A. Hirano, M. Fujita, N. Amir, Y. Miyashita, K. Okamoto. *Inorg. Chim. Acta*, **358**, 667 (2005).

[22] Y. Yamada, K. Okamoto. *Chem. Lett.*, **28**, 315 (1999).

[23] Y. Yamada, K. Fujisawa, K. Okamoto. *Bull. Chem. Soc. Jpn*, **73**, 2297 (2000).